

Supplement of Atmos. Chem. Phys., 18, 3563–3587, 2018
<https://doi.org/10.5194/acp-18-3563-2018-supplement>
© Author(s) 2018. This work is distributed under
the Creative Commons Attribution 4.0 License.



Supplement of

Analysis of the distributions of hourly NO₂ concentrations contributing to annual average NO₂ concentrations across the European monitoring network between 2000 and 2014

Christopher S. Malley et al.

Correspondence to: Christopher S. Malley (chris.malley@york.ac.uk)

The copyright of individual parts of the supplement might differ from the CC BY 4.0 License.

Figure S1: The proportion of within-cluster variance explained as a function of number of clusters for monitoring sites with 2010-2014 average annual NO₂ concentrations between a) 60 and 70 µg m⁻³, b) 50 and 60 µg m⁻³, c) 40 and 50 µg m⁻³, d) 30 and 40 µg m⁻³, e) 20 and 30 µg m⁻³, f) 10 and 20 µg m⁻³, g) 0 and 10 µg m⁻³. The red dot indicates the number of clusters into which sites were grouped.

Figure S2: Map of countries assigned to the European regions used in Figure 3.

Figure S3: Map of sites with 2010-2014 annual NO₂ concentrations (NO_{2AA}) between 60-70 µg m⁻³, grouped into clusters demarcating distinct variations in monthly, hour of day, and hourly NO₂ concentration bin contributions to 2010-2014 NO_{2AA}.

Figure S4: Map of sites with 2010-2014 annual NO₂ concentrations (NO_{2AA}) between 50-60 µg m⁻³, grouped into clusters demarcating distinct variations in monthly, hour of day, and hourly NO₂ concentration bin contributions to 2010-2014 NO_{2AA}.

Figure S5: Map of sites with 2010-2014 annual NO₂ concentrations (NO_{2AA}) between 40-50 µg m⁻³, grouped into clusters demarcating distinct variations in monthly, hour of day, and hourly NO₂ concentration bin contributions to 2010-2014 NO_{2AA}.

Figure S6: Map of sites with 2010-2014 annual NO₂ concentrations (NO_{2AA}) between 30-40 µg m⁻³, grouped into clusters demarcating distinct variations in monthly, hour of day, and hourly NO₂ concentration bin contributions to 2010-2014 NO_{2AA}.

Figure S7: Map of sites with 2010-2014 annual NO₂ concentrations (NO_{2AA}) between 20-30 µg m⁻³, grouped into clusters demarcating distinct variations in monthly, hour of day, and hourly NO₂ concentration bin contributions to 2010-2014 NO_{2AA}.

Figure S8: Map of sites with 2010-2014 annual NO₂ concentrations (NO_{2AA}) between 10-20 µg m⁻³, grouped into clusters demarcating distinct variations in monthly, hour of day, and hourly NO₂ concentration bin contributions to 2010-2014 NO_{2AA}.

Figure S9: Map of sites with 2010-2014 annual NO₂ concentrations (NO_{2AA}) between 0-10 µg m⁻³, grouped into clusters demarcating distinct variations in monthly, hour of day, and hourly NO₂ concentration bin contributions to 2010-2014 NO_{2AA}.

Figure S10: Comparison of the direction and magnitude of the trend in annual NO₂ concentrations between 2000 and 2014 at 259 sites across Europe using the Theil-Sen statistic and first order autoregressive (AR(1)) model.

Figure S11: Magnitude and significance of trend in annual average NO₂ concentrations between 2000 and 2014, with sites separated into panels based on 2010-2014 average annual NO₂ concentrations (NO_{2AA}). The fill colour in each point denotes the magnitude and direction of the Theil-Sen trend at a site, and the outer colour denotes whether the trend was statistically significant ($p \leq 0.05$, green), or not statistically significant ($p > 0.05$, orange). Trend estimates were calculated using the Theil-Sen statistic and block bootstrapping.

Figure S12: Proportion of sites with significant decreasing (blue), increasing (red) ($p \leq 0.05$), and non-significant (grey) trends in the monthly percentage contribution to annual average NO₂ between 2000 and 2014, for sites with 2010-2014 average annual NO₂ concentrations (NO_{2AA}) of a) $>80 \mu\text{g m}^{-3}$, b) $60\text{-}70 \mu\text{g m}^{-3}$, c) $50\text{-}60 \mu\text{g m}^{-3}$, d) $40\text{-}50 \mu\text{g m}^{-3}$, $30\text{-}40 \mu\text{g m}^{-3}$, $20\text{-}30 \mu\text{g m}^{-3}$, $10\text{-}20 \mu\text{g m}^{-3}$, $0\text{-}10 \mu\text{g m}^{-3}$. Trend estimates were calculated using the Theil-Sen statistic and block bootstrapping. The black line represents the division between decreasing and increasing trends within the non-significant bar.

Figure S13: Proportion of sites with significant decreasing (blue), increasing (red) ($p \leq 0.05$), and non-significant (grey) trends in the percentage contribution of each hour of day to annual average NO₂ between 2000 and 2014, for sites with 2010-2014 average annual NO₂ concentrations (NO_{2AA}) of a) $>80 \mu\text{g m}^{-3}$, b) $60\text{-}70 \mu\text{g m}^{-3}$, c) $50\text{-}60 \mu\text{g m}^{-3}$, d) $40\text{-}50 \mu\text{g m}^{-3}$, $30\text{-}40 \mu\text{g m}^{-3}$, $20\text{-}30 \mu\text{g m}^{-3}$, $10\text{-}20 \mu\text{g m}^{-3}$, $0\text{-}10 \mu\text{g m}^{-3}$. Trend estimates were calculated using the Theil-Sen statistic and block bootstrapping. The black line represents the division between decreasing and increasing trends within the non-significant bar.

Figure S14: Proportion of sites with significant decreasing (blue), increasing (red) ($p < 0.05$), and non-significant (grey) trends in the percentage contribution from hourly NO₂ concentrations in $5 \mu\text{g m}^{-3}$ bins to annual average NO₂ between 2000 and 2014, for sites with 2010-2014 average annual NO₂ concentrations (NO_{2AA}) of a) $>80 \mu\text{g m}^{-3}$, b) $60\text{-}70 \mu\text{g m}^{-3}$, c) $50\text{-}60 \mu\text{g m}^{-3}$, d) $40\text{-}50 \mu\text{g m}^{-3}$, $30\text{-}40 \mu\text{g m}^{-3}$, $20\text{-}30 \mu\text{g m}^{-3}$, $10\text{-}20 \mu\text{g m}^{-3}$, $0\text{-}10 \mu\text{g m}^{-3}$. Trend estimates were calculated using the Theil-Sen statistic and block bootstrapping. The black line represents the division between decreasing and increasing trends within the non-significant bar.

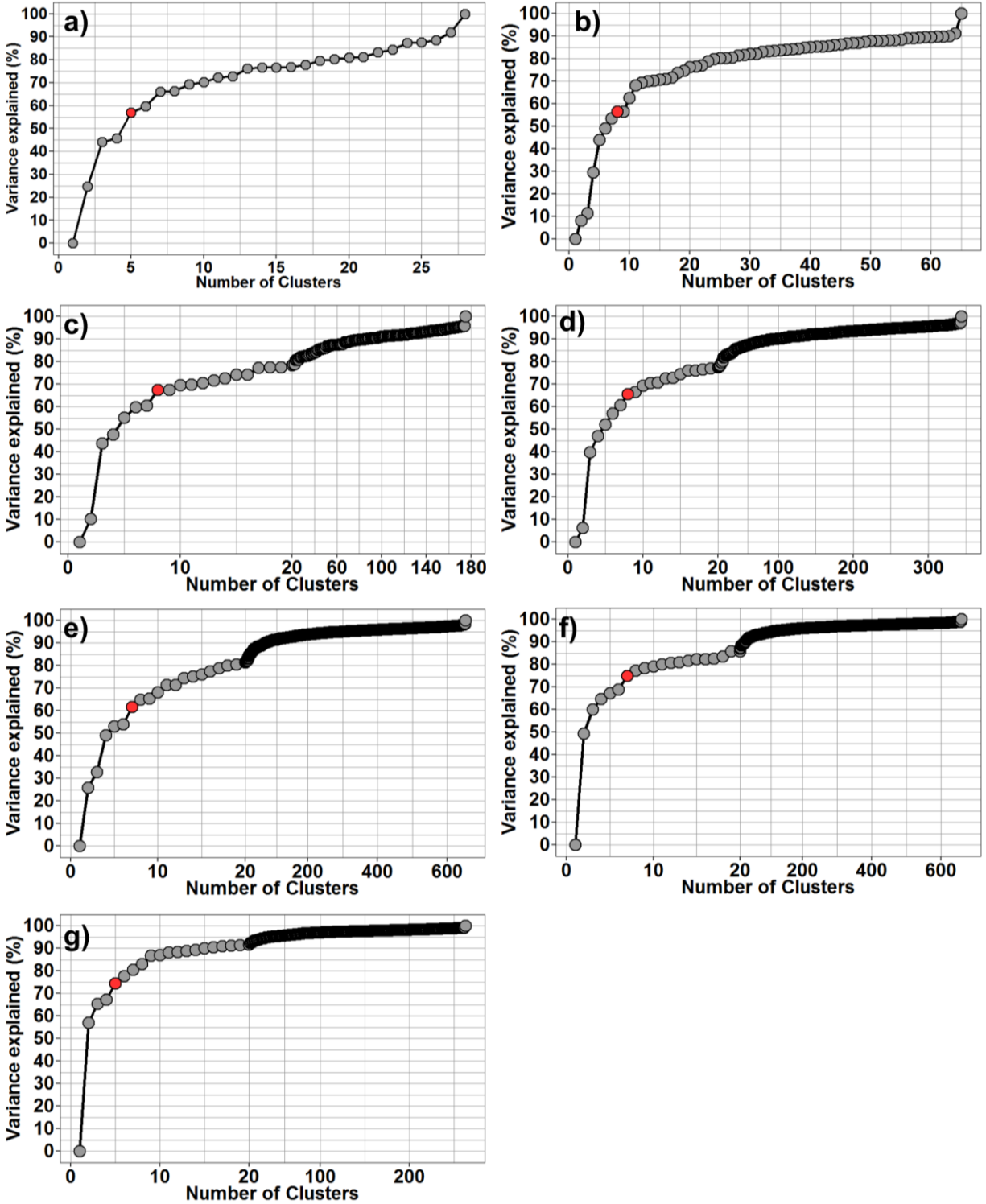


Figure S1: The proportion of within-cluster variance explained as a function of number of clusters for monitoring sites with 2010-2014 average annual NO₂ concentrations between a) 60 and 70 μg m⁻³, b) 50 and 60 μg m⁻³, c) 40 and 50 μg m⁻³, d) 30 and 40 μg m⁻³, e) 20 and 30 μg m⁻³, f) 10 and 20 μg m⁻³, g) 0 and 10 μg m⁻³. The red dot indicates the number of clusters into which sites were grouped.

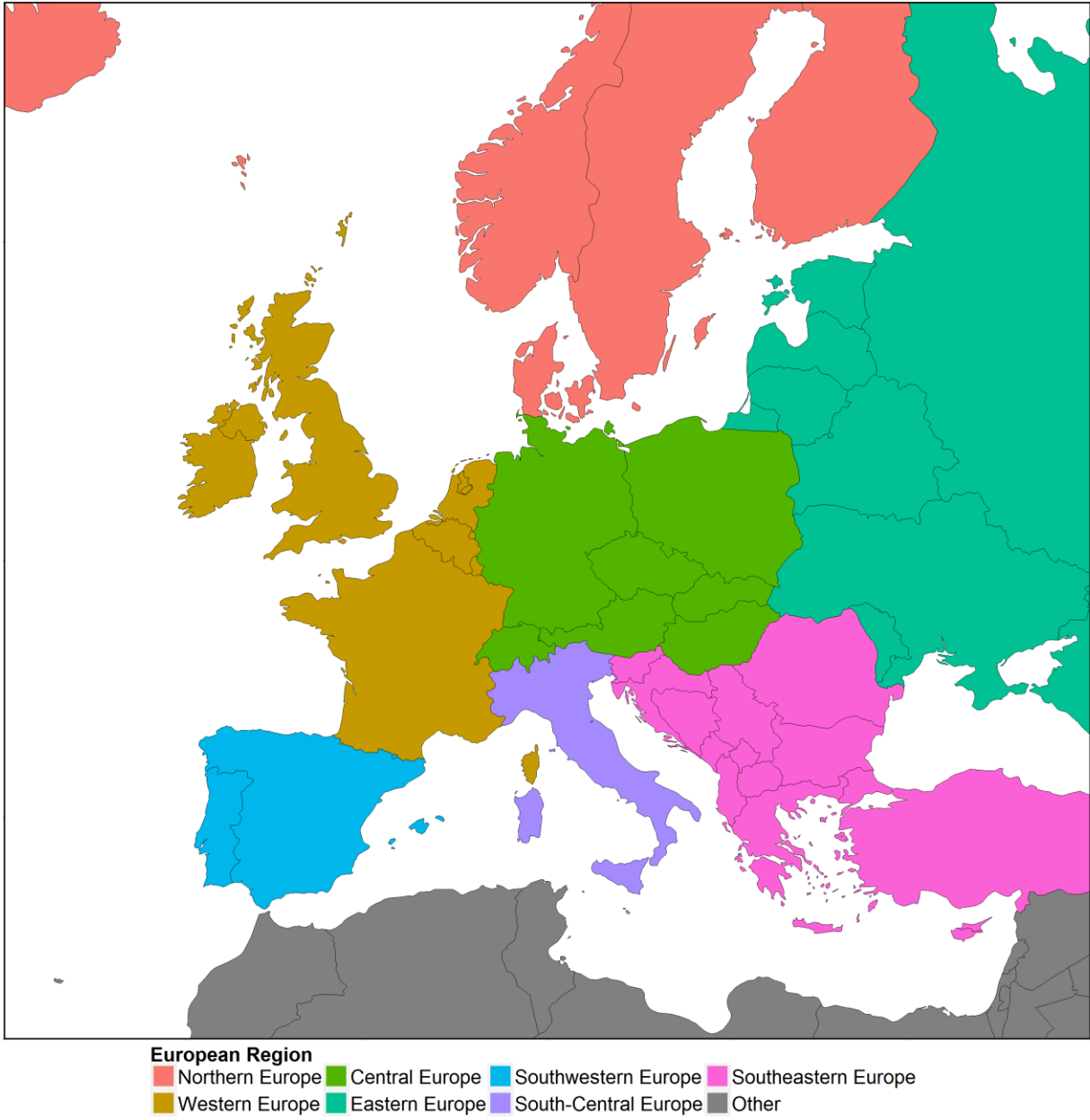


Figure S2: Map of countries assigned to the European regions used in Figure 3.

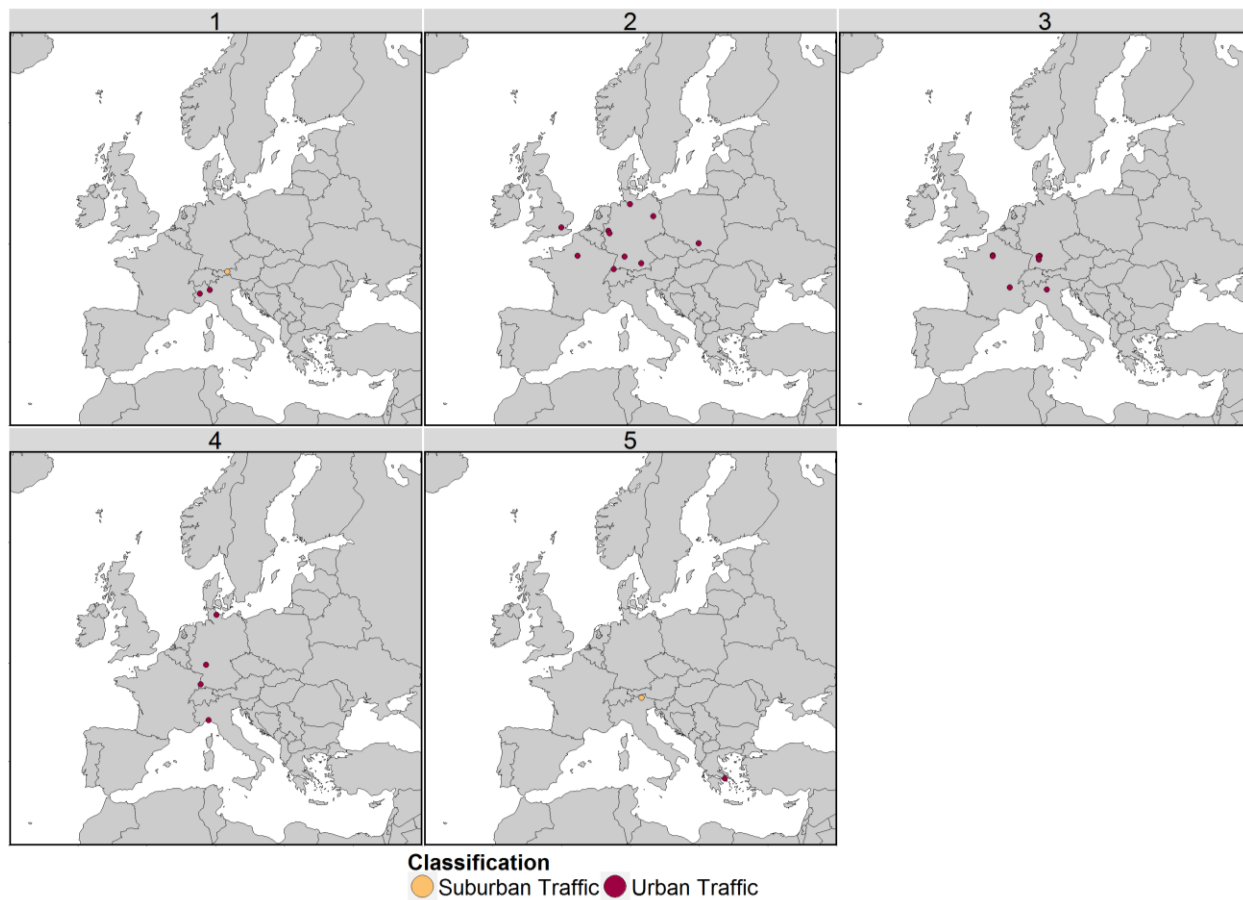


Figure S3: Map of sites with 2010-2014 annual NO_2 concentrations ($\text{NO}_{2\text{AA}}$) between $60\text{--}70 \mu\text{g m}^{-3}$, grouped into clusters demarcating distinct variations in monthly, hour of day, and hourly NO_2 concentration bin contributions to 2010-2014 $\text{NO}_{2\text{AA}}$.



Classification

● Rural Traffic
 ● Suburban Traffic
 ● Urban Background
 ● Urban Industrial
 ● Urban Traffic

Figure S4: Map of sites with 2010-2014 annual NO_2 concentrations ($\text{NO}_{2\text{AA}}$) between $50\text{-}60 \mu\text{g m}^{-3}$, grouped into clusters demarcating distinct variations in monthly, hour of day, and hourly NO_2 concentration bin contributions to 2010-2014 $\text{NO}_{2\text{AA}}$.

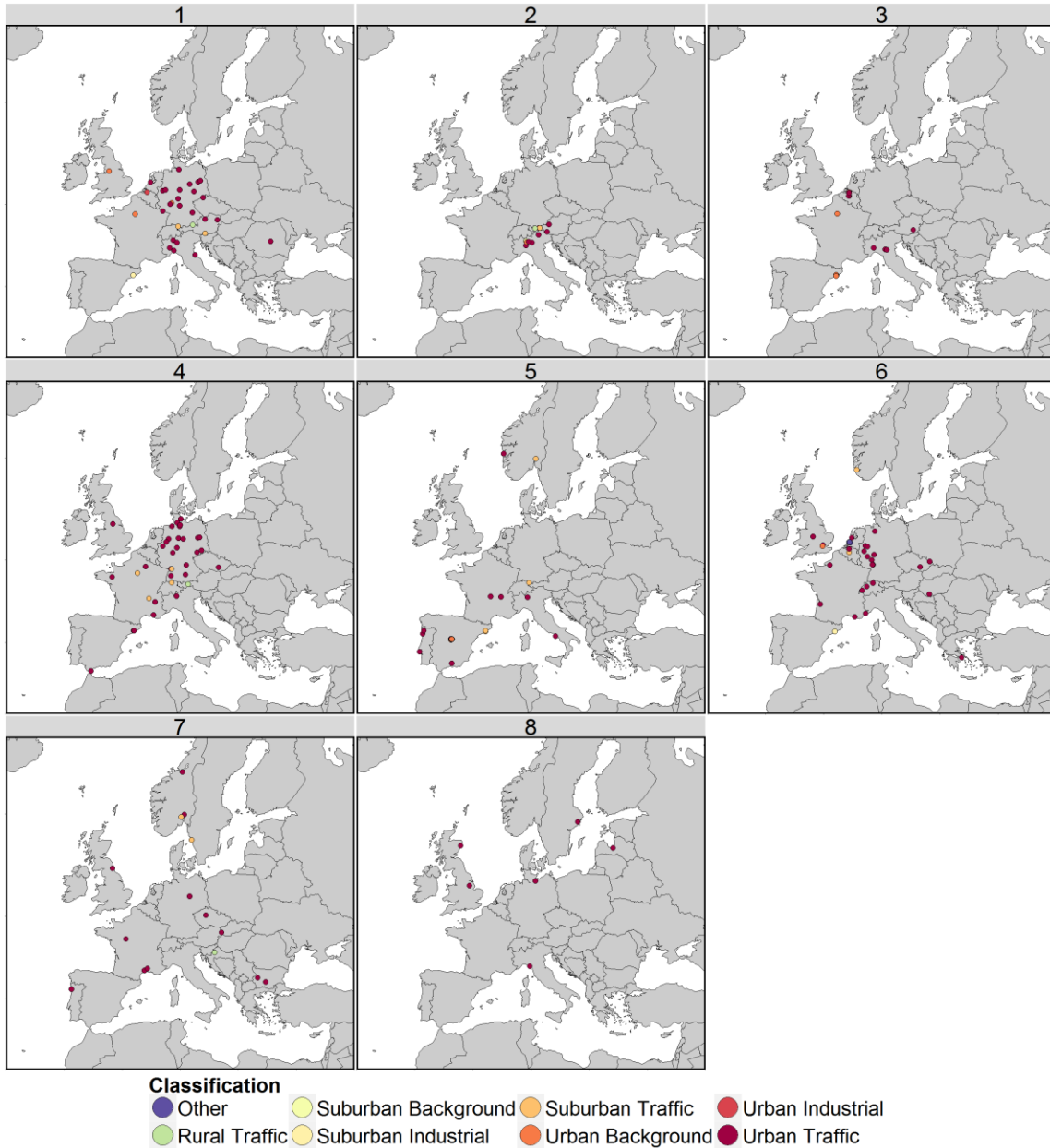
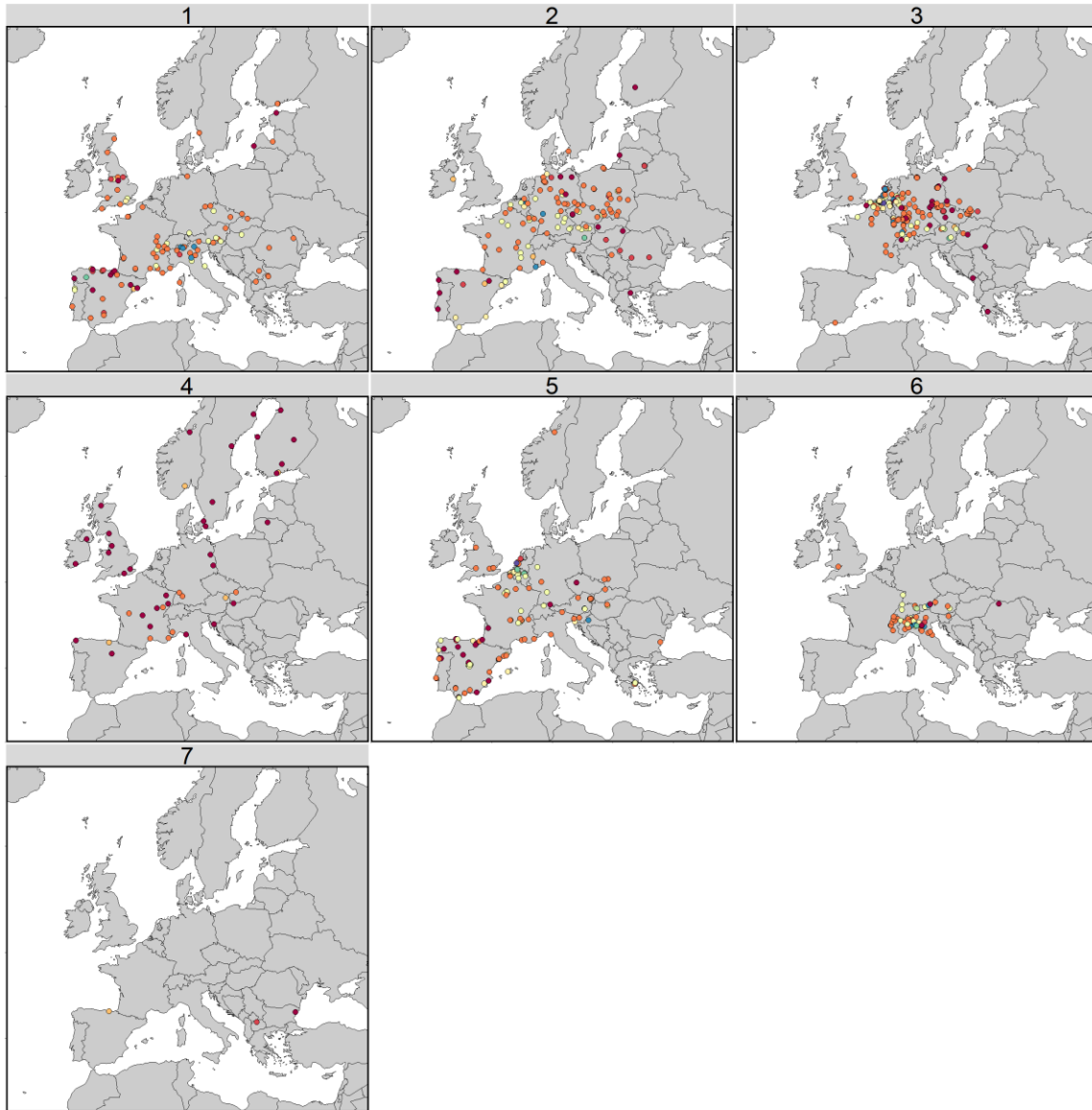


Figure S5: Map of sites with 2010-2014 annual NO_2 concentrations ($\text{NO}_{2\text{AA}}$) between $40\text{-}50 \mu\text{g m}^{-3}$, grouped into clusters demarcating distinct variations in monthly, hour of day, and hourly NO_2 concentration bin contributions to 2010-2014 $\text{NO}_{2\text{AA}}$.



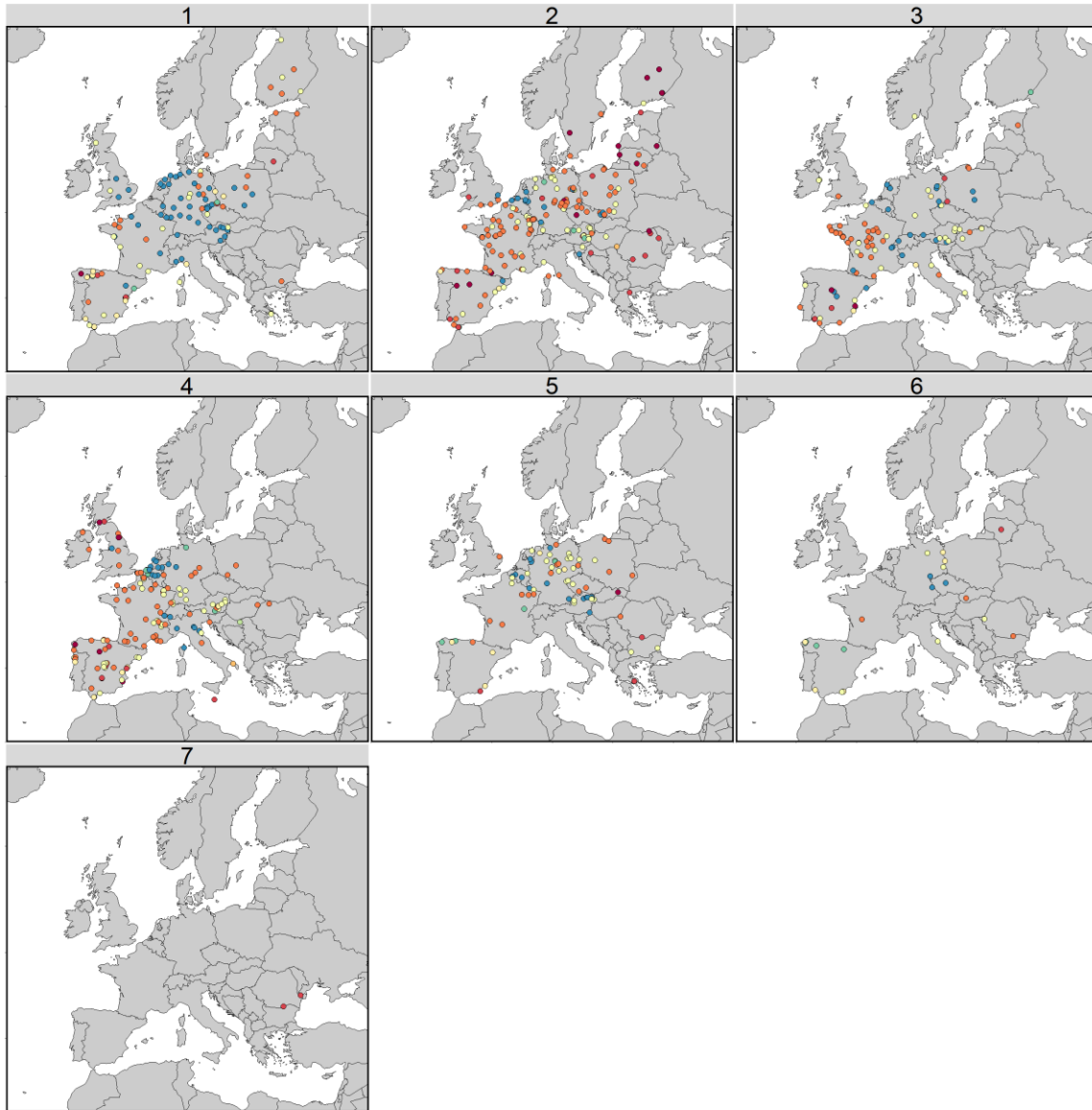
Figure S6: Map of sites with 2010-2014 annual NO_2 concentrations ($\text{NO}_{2\text{AA}}$) between $30\text{--}40 \mu\text{g m}^{-3}$, grouped into clusters demarcating distinct variations in monthly, hour of day, and hourly NO_2 concentration bin contributions to 2010-2014 $\text{NO}_{2\text{AA}}$.



Classification

● Other	● Rural Industrial	● Suburban Background	● Suburban Traffic	● Urban Industrial
● Rural Background	● Rural Traffic	● Suburban Industrial	● Urban Background	● Urban Traffic

Figure S7: Map of sites with 2010-2014 annual NO₂ concentrations (NO_{2AA}) between 20-30 μg m⁻³, grouped into clusters demarcating distinct variations in monthly, hour of day, and hourly NO₂ concentration bin contributions to 2010-2014 NO_{2AA}.



Classification

● Other	● Rural Industrial	● Suburban Background	● Suburban Traffic	● Urban Industrial
● Rural Background	● Rural Traffic	● Suburban Industrial	● Urban Background	● Urban Traffic

Figure S8: Map of sites with 2010-2014 annual NO_2 concentrations ($\text{NO}_{2\text{AA}}$) between $10\text{-}20 \mu\text{g m}^{-3}$, grouped into clusters demarcating distinct variations in monthly, hour of day, and hourly NO_2 concentration bin contributions to 2010-2014 $\text{NO}_{2\text{AA}}$.

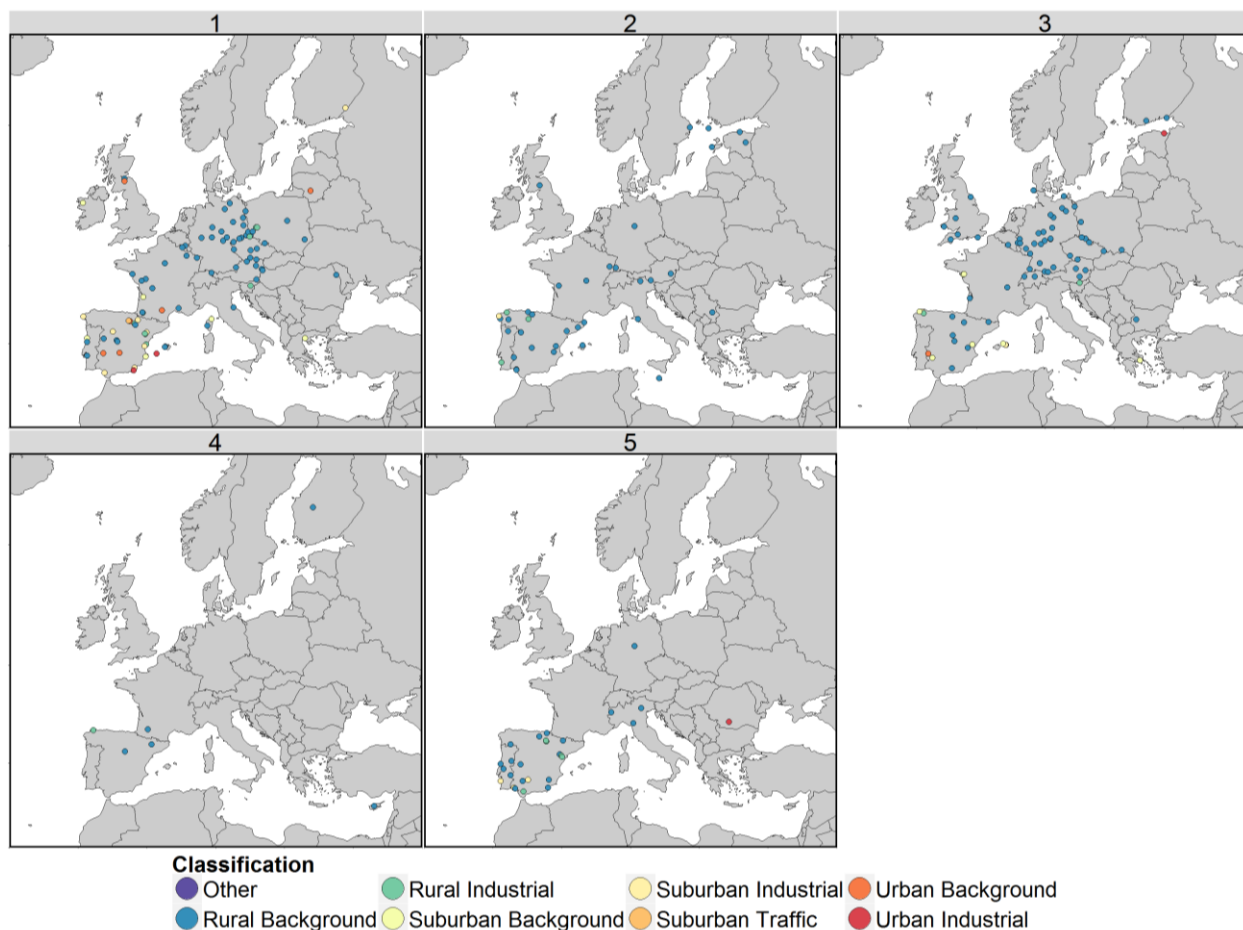


Figure S9: Map of sites with 2010-2014 annual NO_2 concentrations ($\text{NO}_{2\text{AA}}$) between $0\text{-}10 \mu\text{g m}^{-3}$, grouped into clusters demarcating distinct variations in monthly, hour of day, and hourly NO_2 concentration bin contributions to 2010-2014 $\text{NO}_{2\text{AA}}$.

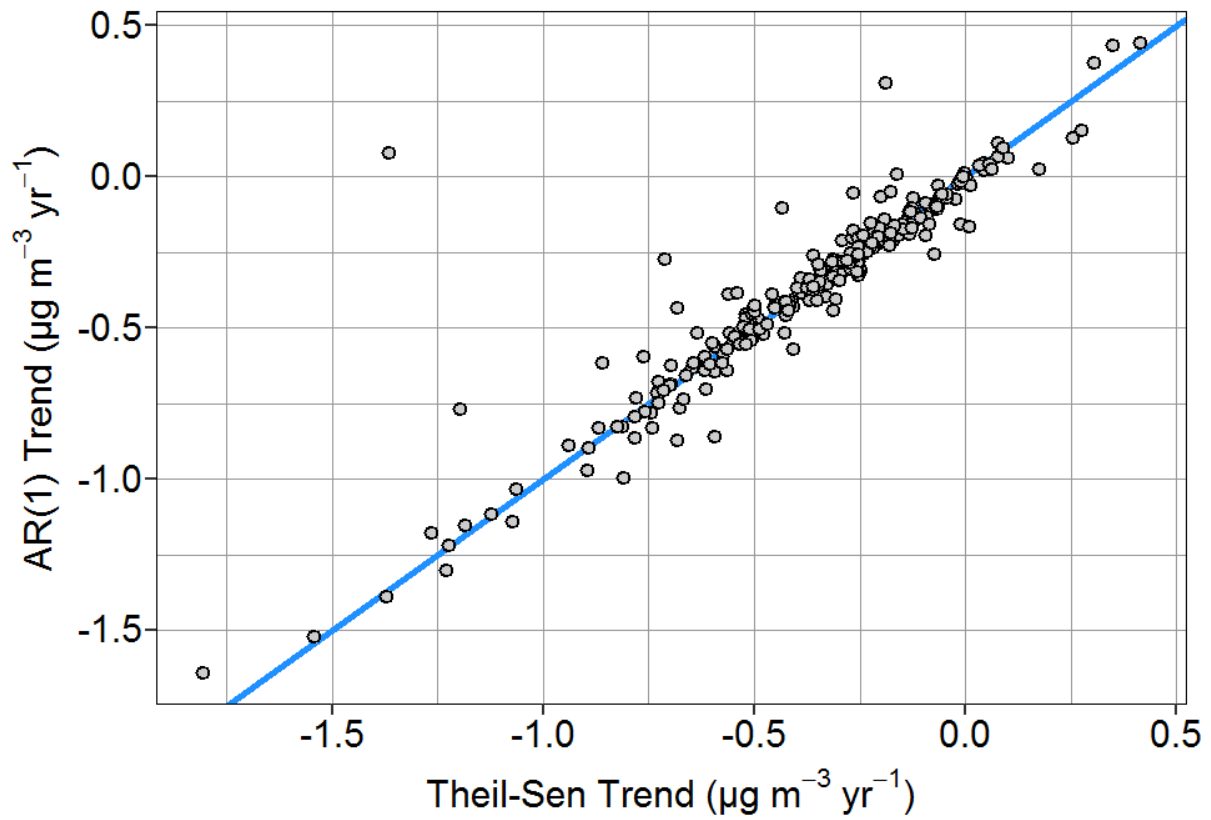


Figure S10: Comparison of the direction and magnitude of the trend in annual NO₂ concentrations between 2000 and 2014 at 259 sites across Europe using the Theil-Sen statistic and first order autoregressive (AR(1)) model.

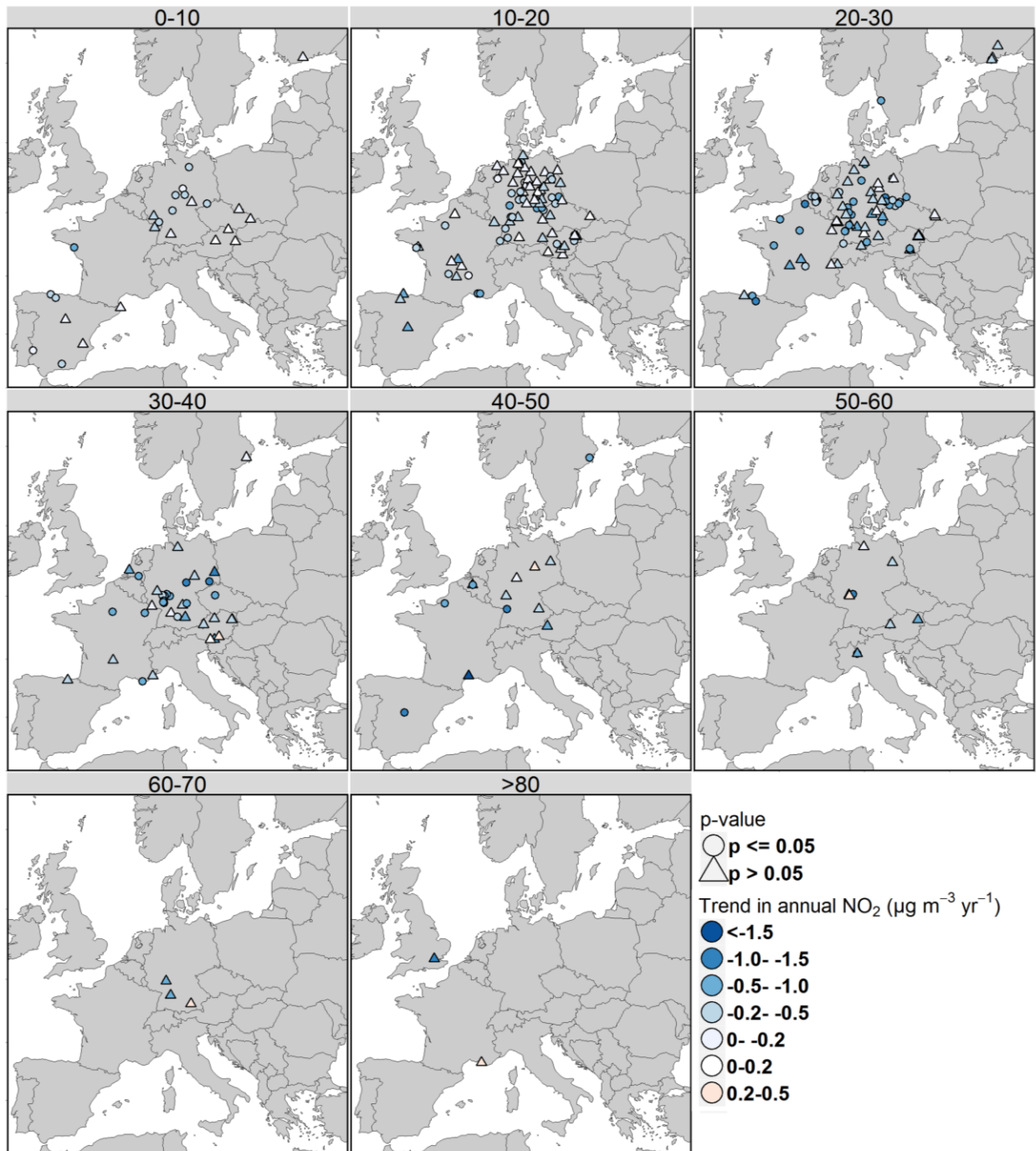


Figure S11: Magnitude and significance of trend in annual average NO₂ concentrations between 2000 and 2014, with sites separated into panels based on 2010-2014 average annual NO₂ concentrations (NO_{2AA}). The fill colour in each point denotes the magnitude and direction of the Theil-Sen trend at a site, and the outer colour denotes whether the trend was statistically significant ($p \leq 0.05$, green), or not statistically significant ($p > 0.05$, orange). Trend estimates were calculated using the Theil-Sen statistic and block bootstrapping.

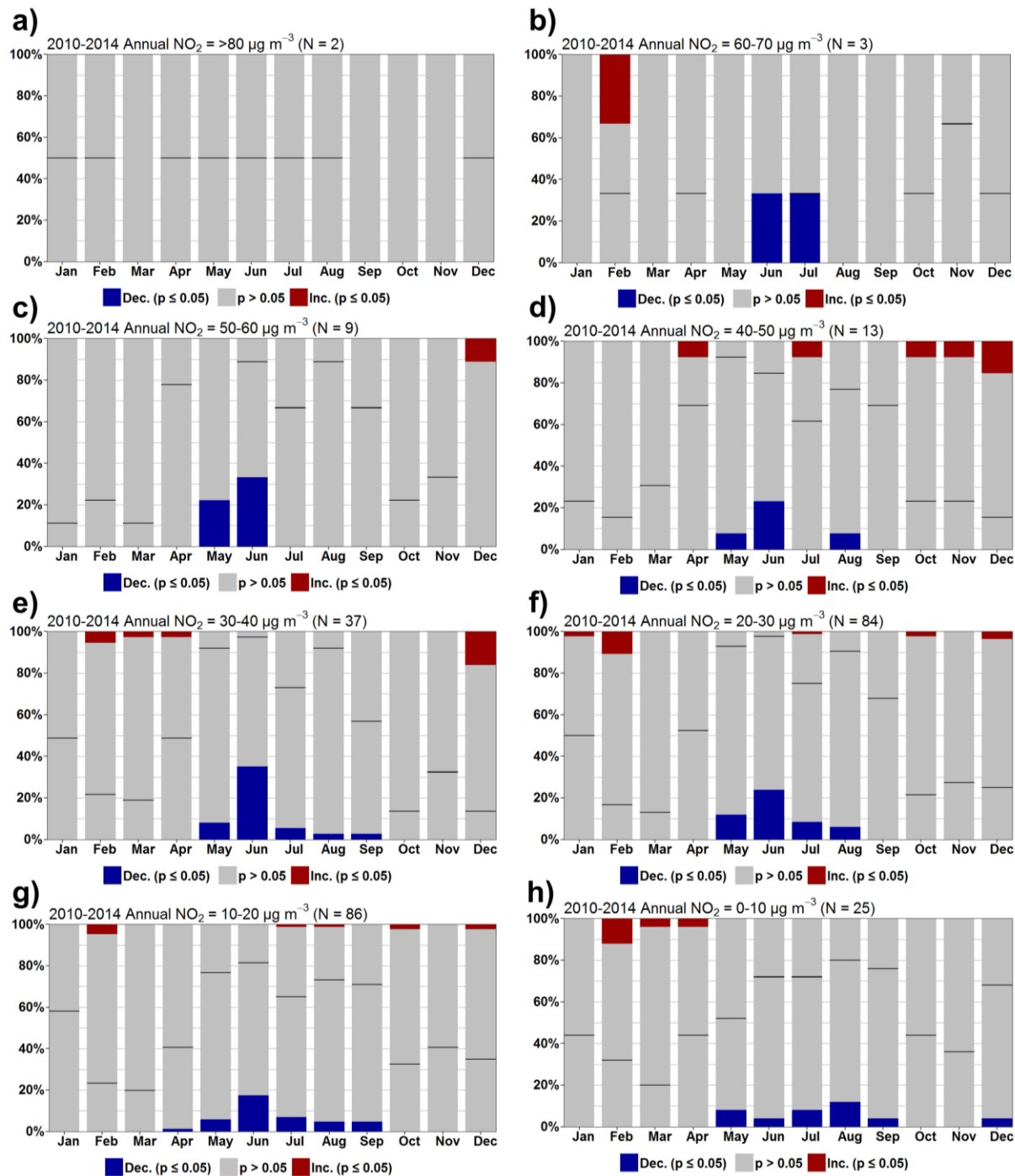


Figure S12: Proportion of sites with significant decreasing (blue), increasing (red) ($p \leq 0.05$), and non-significant (grey) trends in the monthly percentage contribution to annual average NO_2 between 2000 and 2014, for sites with 2010-2014 average annual NO_2 concentrations ($\text{NO}_{2\text{AA}}$) of a) $>80 \mu\text{g m}^{-3}$, b) $60\text{-}70 \mu\text{g m}^{-3}$, c) $50\text{-}60 \mu\text{g m}^{-3}$, d) $40\text{-}50 \mu\text{g m}^{-3}$, $30\text{-}40 \mu\text{g m}^{-3}$, $20\text{-}30 \mu\text{g m}^{-3}$, $10\text{-}20 \mu\text{g m}^{-3}$, $0\text{-}10 \mu\text{g m}^{-3}$. Trend estimates were calculated using the Theil-Sen statistic and block bootstrapping. The black line represents the division between decreasing and increasing trends within the non-significant bar.

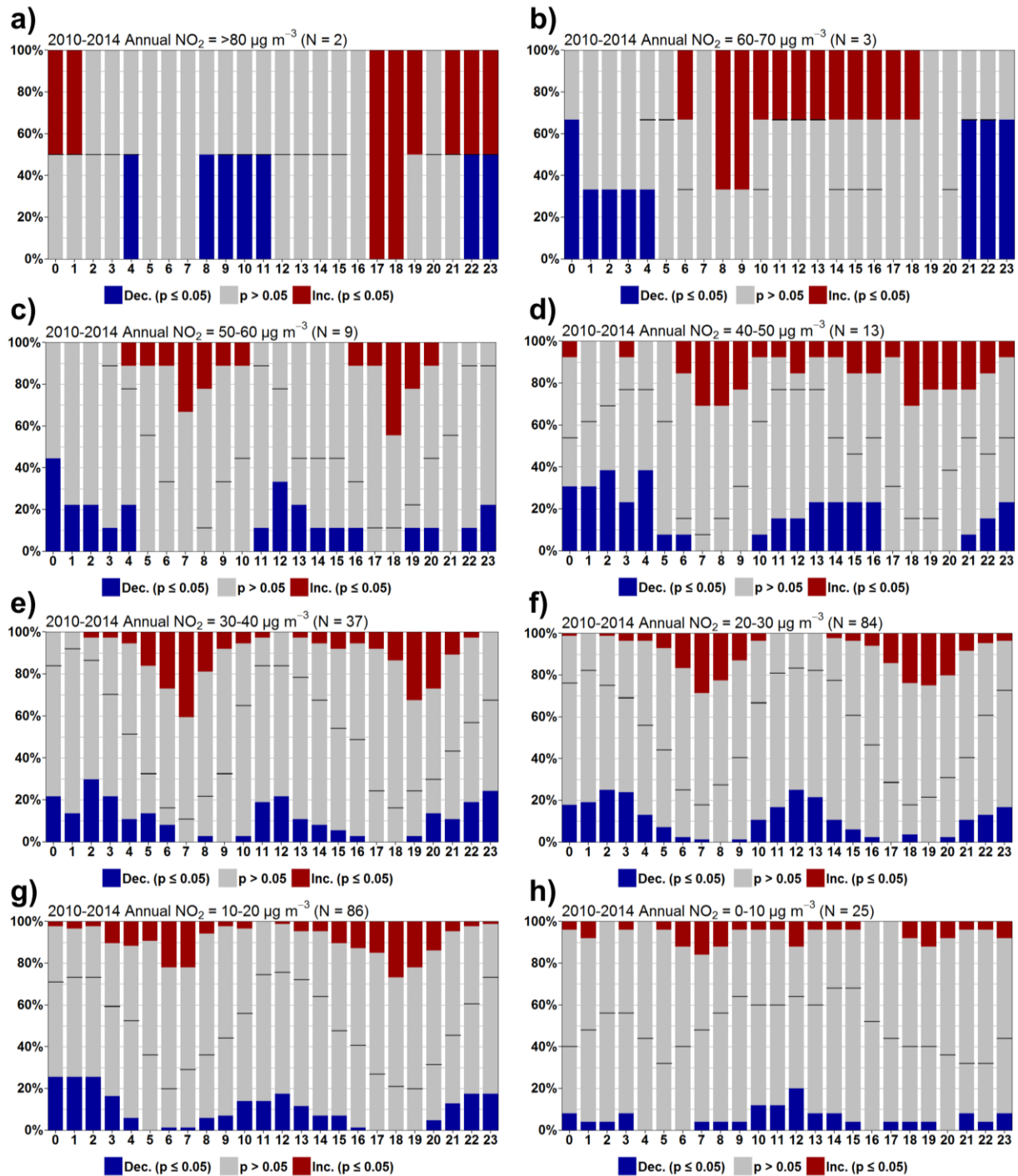


Figure S13: Proportion of sites with significant decreasing (blue), increasing (red) ($p \leq 0.05$), and non-significant (grey) trends in the percentage contribution of each hour of day to annual average NO_2 between 2000 and 2014, for sites with 2010-2014 average annual NO_2 concentrations ($\text{NO}_{2\text{AA}}$) of a) $>80 \mu\text{g m}^{-3}$, b) $60\text{-}70 \mu\text{g m}^{-3}$, c) $50\text{-}60 \mu\text{g m}^{-3}$, d) $40\text{-}50 \mu\text{g m}^{-3}$, e) $30\text{-}40 \mu\text{g m}^{-3}$, f) $20\text{-}30 \mu\text{g m}^{-3}$, g) $10\text{-}20 \mu\text{g m}^{-3}$, h) $0\text{-}10 \mu\text{g m}^{-3}$. Trend estimates were calculated using the Theil-Sen statistic and block bootstrapping. The black line represents the division between decreasing and increasing trends within the non-significant bar.

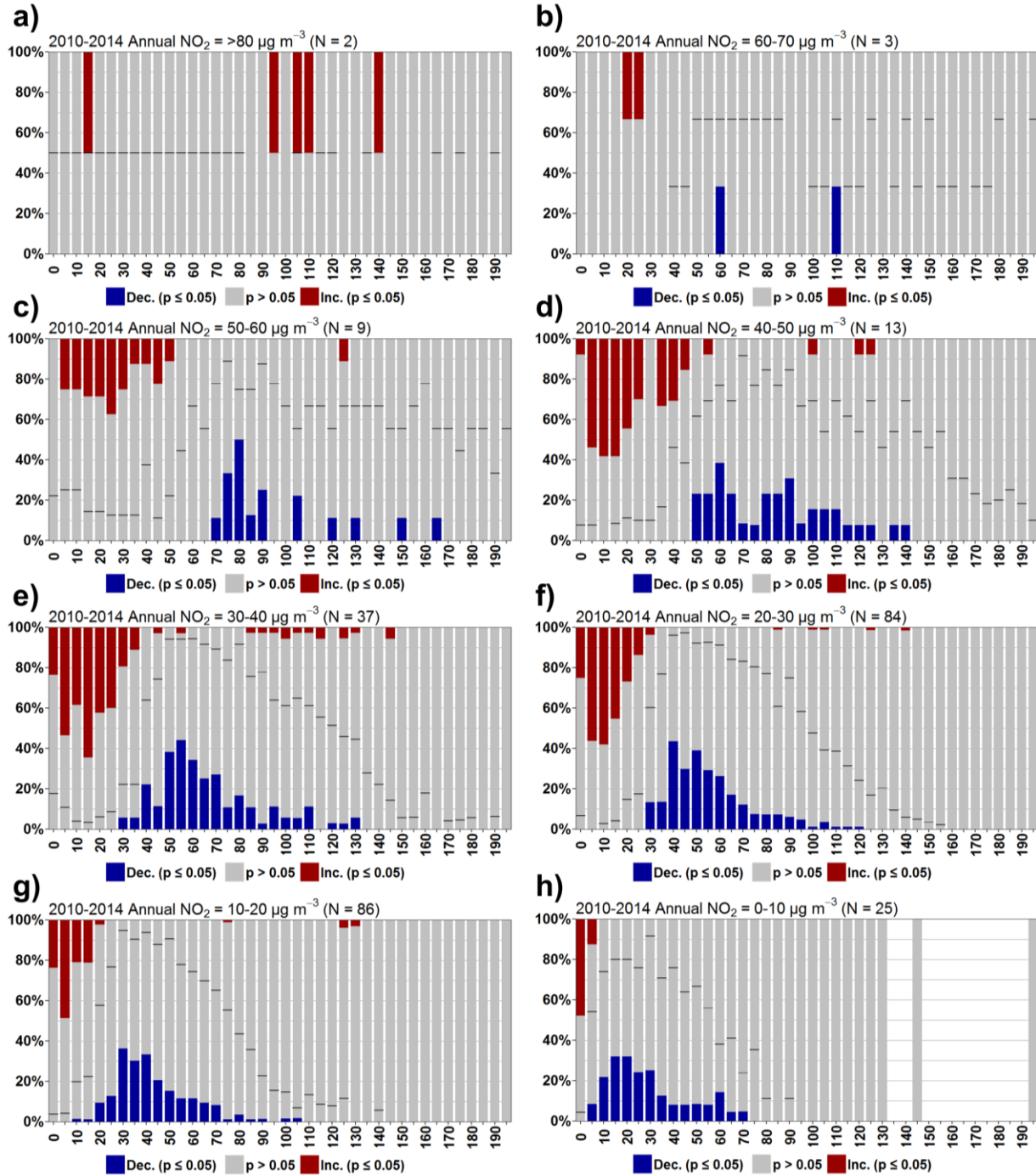


Figure S14: Proportion of sites with significant decreasing (blue), increasing (red) ($p < 0.05$), and non-significant (grey) trends in the percentage contribution from hourly NO_2 concentrations in $5 \mu g m^{-3}$ bins to annual average NO_2 between 2000 and 2014, for sites with 2010-2014 average annual NO_2 concentrations (NO_{2AA}) of a) $>80 \mu g m^{-3}$, b) $60-70 \mu g m^{-3}$, c) $50-60 \mu g m^{-3}$, d) $40-50 \mu g m^{-3}$, e) $30-40 \mu g m^{-3}$, f) $20-30 \mu g m^{-3}$, g) $10-20 \mu g m^{-3}$, h) $0-10 \mu g m^{-3}$. Trend estimates were calculated using the Theil-Sen statistic and block bootstrapping. The black line represents the division between decreasing and increasing trends within the non-significant bar.